ARTICLE

Macroscopic Frictional Properties of Poly(1-(2-methacryloyloxy)ethyl-3-butyl Imidazolium Bis(trifluoromethanesulfonyl)-imide) Brush Surfaces in an Ionic Liquid

Tatsuya Ishikawa,[†] Motoyasu Kobayashi,[‡] and Atsushi Takahara*[,†,‡,§]

Graduate School of Engineering, Kyushu University, Japan Science and Technology Agency, ERATO, Takahara Soft Interfaces Project, and Institute for Materials Chemistry and Engineering, Kyushu University, 744 Motooka, Nishi-ku, Fukuoka 819-0395, Japan

ABSTRACT Poly(1-(2-methacryloyloxy)ethyl-3-butylimidazolium bis(trifluoromethanesulfonyl)imide) (PMIS) and poly(*n*-hexyl methacrylate) (PHMA) brushes were prepared on initiator-immobilized silicon wafers by surface-initiated atom transfer radical polymerization. The macroscopic frictional properties of the brushes were determined using a ball-on-flat type tribotester under reciprocating motion in a dry nitrogen atmosphere, water, methanol, and 1-ethyl-3-methylimidazolium bis(trifluoromethanesulfonyl)imide (EMImTFSI). When the PMIS and PHMA brushes were exposed to EMImTFSI, the friction coefficient of the former was lower than that of the latter. It is thought that the high affinity of the PMIS brush to EMImTFSI led to a reduction in the interaction between the brush and the friction probe, which resulted in a low friction coefficient. The friction force of the PMIS brush in EMImTFSI was proportional to a normal load in the range of 0.2−0.98 N. The friction coefficient gradually decreased to 0.01 with an increase in the sliding velocity from 1×10^{-4} to 1×10^{-1} m s^{-1}. The friction coefficient of the PMIS brush exhibited low magnitude until 800 friction cycles in the dry nitrogen atmosphere, whereas the PHMA brush was abraded away within 150 friction cycles. The XPS spectra of the worn surfaces on the PMIS brush suggested that the brush was gradually abraded by friction.

KEYWORDS: ionic liquid • polymer brush • tribology • friction coefficient • surface-initiated polymerization

INTRODUCTION

Since Liu et al. first reported the use of room-temperature ionic liquids as novel lubricants (1−3), ionic liquids have attracted much attention as a new class of lubricants (4, 5) because of their unique properties such as negligible volatility, low flammability, high thermal stability (6), a low melting point, and a wide liquid range (7). These characteristics are derived from ionic interactions between organic cations and noncoordinating anions, which together form salts with low melting points around room temperature (8). Ionic liquids are expected to be ideal candidates for new lubricants under severe conditions such as ultrahigh vacuum and extreme temperatures (9, 10). Actually, ionic liquids have lower friction coefficients and better wear resistance than conventional lubricants such as synthetic hydrocarbons and fluoroether polymers (1), although such tribological properties are largely dependent on the chemical structure of the organic cations and anions (11). Liu et al. proposed that ionic liquids could be easily adsorbed on the sliding surfaces of frictional pairs because of their polar structure; these liquids can form a boundary film, which would effectively reduce friction and wear (1−3). These authors further suggested that a tribochemical reaction (12, 13) between an ionic liquid and a friction surface under severe friction conditions forms protective tribolayers, which was confirmed by Mori and his co-workers. However, a tribochemical reaction involving the decomposition of the ionic liquid would cause corrosive wear (14). In the case of an *N*-alkyl imidazolium derivative ionic liquid, it has been reported that imidazolium with a short alkyl chain and a reactive anion, such as tetrafluoroborate BF_4^- and hexafluorophosphate PF_6^-, increased wear through tribocorrosive attack on steel and aluminum surfaces (15). One of the reasons for the increased wear is that BF_4^- and PF_6^- afford corrosive hydrogen fluoride upon hydrolysis, which can damage tribological systems (16). Jiménez et al. reported that trifluoromethanesulfonate or 4-methylbenzenesulfonate anions can reduce tribocorrosion and consequently, friction and wear, despite the presence of the short alkyl chains of the imidazolium cation (17). In contrast, BF_4^- of imidazolium cations with long alkyl chains results in lower friction and wear compared to the corresponding PF_6^- salt (17, 18). The pressure viscosity coefficient of ionic liquids is also an important factor in the formation of a lubrication film. Therefore, the lubrication film for hydrodynamic lubrication and the boundary layer on the friction surface are important for reducing friction and wear using ionic liquids as well as conventional oil-base lubricants. In this study, we propose

* Corresponding author. Phone: +81-92-802-2517. Fax: +81-92-802-2518. E-mail: takahara@cstf.kyushu-u.ac.jp.
Received for review December 20, 2009 and accepted March 29, 2010
[†] Graduate School of Engineering, Kyushu University.
[‡] Japan Science and Technology Agency, ERATO.
[§] Institute for Materials Chemistry and Engineering, Kyushu University.
DOI: 10.1021/am9009082

Published on Web 04/06/2010

another type of boundary layer prepared by grafting a polymer film consisting of an ionic liquid moiety on the friction surface to improve the tribological properties.

Grafting a polymer or alkyl chains on a solid surface is a promising surface-modification method for controlling the surface wettability, adhesion, and tribological properties (19−21). Generally, polymer chains tethered to a surface with sufficiently high grafting density are called "polymer brushes" (22). The densely grafted brush chains assume a highly extended conformation in a good solvent due to the osmotic pressure. The equilibrium thickness of swollen brushes is determined by the balance between the osmotic pressure and extensional stress of the chains. The reduction in the friction forces between solid surfaces bearing polymer brushes, especially in a good solvent, has been studied well, both theoretically (23, 24) and experimentally (25−28). The efficient lubrication of the solvated brushes is attributed to the osmotic pressure of the compressed chains, together with the weak interpenetration of the two brushes (29). Klein et al. have studied the normal and shear forces (26) between opposing polystyrene (PS) brushes immersed in toluene using a surface force apparatus (SFA), although the brushes were prepared by the "grafting to" method. The brushes were found to function as an extremely efficient lubricant up to a moderate pressure because the interpenetration between opposing brushes was suppressed by configurational entropy effects (26, 29, 30). At much higher compressions, larger shear forces are observed because of the mutual interpenetration of the brushes and the elastic stretching of the chains when their tethered ends begin to move laterally (31). When the shear rate is increased to an extent where it is comparable to the relaxation rate of the chain segments, the opposing chains in the interfacial region do not become entangled; this is due to a self-regulating mechanism, resulting in lower shear forces. In a theta solvent, large shear forces can be detected even at milder levels of compression (32), due to changes in the strength of the frictional interaction (30), interpenetrating depth (33), and vitrification of the compressed polymer layers (27, 34, 35). Kilbey et al. have investigated the influence of polymer-solvent interactions on the frictional properties of PS brushes in cyclohexane at various temperatures (36).

Tsujii et al. reported the tribological properties of high-density poly(methyl methacrylate) (PMMA) brushes in toluene; the brushes were prepared by surface-initiated atom transfer radical polymerization (SI-ATRP) (37). These authors measured the interaction force between the graft layer and a silica probe attached to an atomic force microscope (AFM) cantilever and found that a large osmotic pressure leads to the extension of the grafted polymer chains in the vertical direction, giving rise to an extremely strong resistance to normal force loading (38). The steric repulsion between polymer brushes supporting high normal loads results in low frictional forces between the brush-bearing surfaces (38). The macroscopic frictional properties of high-density PMMA brush were also investigated by Takahara et al. (39) They showed that PMMA brushes could be used as very effective lubricants between sliding surfaces immersed in a good solvent.

Therefore, a high-density polymer brush bearing ionic liquid moieties is expected to act as a good boundary layer. In fact, two types of poly(ionic liquid) brushes have already been synthesized. Yu et al. prepared a poly(1-ethyl 3-(2-methacryloyloxy ethyl) imidazolium chloride) brush on a gold surface and investigated its swelling/collapsing behavior in different electrolyte solutions and its electrochemical properties (40). Yang et al. prepared a PS brush with an imidazolium hexafluorophosphate unit in the side chain by SI-ATRP (41). They found that the surface wettability of poly(ionic liquid) brushes can be controlled by exchanging their counteranions. In this study, a poly(methacrylate) brush bearing an *N*-alkylimidazolium-type ionic liquid unit in the side chain was prepared on a silicon wafer by SI-ATRP. To achieve low friction and inhibit corrosive wear, we selected a combination of an *n*-butyl group and bis(trifluoromethanesulfonyl)imide (TFSI) as the *N*-alkyl chain for the imidazolium and counteranions. Subsequently, the macrotribological properties of poly(1-(2-methacryloyloxy)ethyl-3-butylimidazolium bis(trifluoromethanesulfonyl)imide) (PMIS) brushes in a dry nitrogen atmosphere, water, methanol, and an ionic liquid were investigated. A tribotest of the poly(*n*-hexyl methacrylate) (PHMA) brush surface was also carried out as a control experiment.

EXPERIMENTAL SECTION

Materials. Copper(I) bromide (CuBr, Wako Pure Chemicals (Wako), 99.9%) was purified by successive washing with acetic acid and ethanol and was dried in a vacuum. Acetonitrile (Wako, 99.5%), ethyl 2-bromoisobutylate (EB, Tokyo Chemical Inc. (TCI), 98%), *n*-hexyl methacrylate (TCI, 98%), and pyridine (Wako, 99.5%) were dried and distilled over CaH_2 before use. Commercially available 2-bromoethanol (TCI, 95%), *N*-butylimidazole (Wako), 2,2′-bipyridyl (bpy, Wako, 99.5%), lithium bis(trifluoromethanesulfonyl)imide (LiTFSI, Wako, 98%), and 1-ethyl-3-methylimidazolium bis(trifluoromethanesulfonyl)imide (EMImTFSI, Kanto Chemical Co., Inc., 98%) were used without further purification. Dichloromethane (Kishida Chemical, 99.5%) was purified by passing it through the columns of a Glass Contour Solvent Systems (Hansen Co.) under a high-quality argon gas atmosphere. The procedure used for the synthesis of (2-bromo-2-methyl)propionyloxyhexyltriethoxysilane (BHE) has been described in previous papers (42, 43). The BHE monolayer was immobilized on a silicon wafer by the chemical vapor adsorption technique (44, 45). 2-Bromoethyl methacrylate was synthesized by reacting 2-bromoethanol and methacryloyl chloride in the presence of pyridine in dichloromethane at 273 K, as shown in Scheme 1. Deionized water used for contact angle measurement was purified with the NanoPure Water system (Millipore Inc.).

Synthesis of 1-(2-Methacryloyloxy)ethyl-3-butylimidazolium Bromide (MIB). A mixture of 2-bromoethyl methacrylate (109 mmol) and *N*-butylimidazole (110 mmol) was stirred at 313 K for 4 days. During the reaction, a small amount of *p-tert*-butylcatechol (50 mg) was added to the reaction mixture to inhibit the thermal polymerization of the resulting monomer MIB. The reaction was traced by thin-layer chromatography. The reaction mixture was dissolved in ca. 10 mL of dichloromethane and poured into a large amount of hexane to give a precipitate. The product was collected and dried in vacuo to form a highly

Scheme 1. Preparation of MIS Monomer

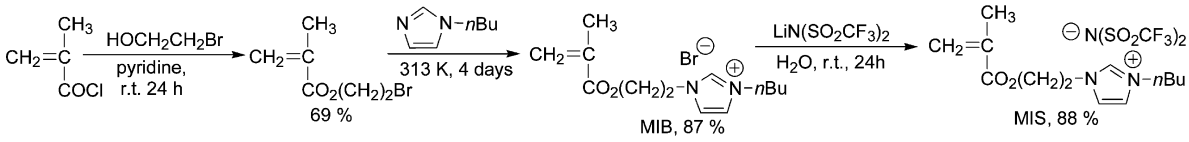

viscous pale-yellow liquid in a yield of 30.16 g (95 mmol, 87%). ^{1}H NMR (DMSO-d_6, 300 MHz): δ 0.87 (t, 3H, $NCH_2CH_2CH_2CH_3$), 1.20 (m, 2H, $NCH_2CH_2CH_2CH_3$), 1.74 (m, 2H, $NCH_2CH_2CH_2CH_3$), 1.82 (s, 3H, CH_3), 4.17 (m, 2H, OCH_2), 4.47 (m, 2H, $NCH_2CH_2CH_2CH_3$), 4.52 (m, 2H, OCH_2CH_2), 5.71 and 6.01 (s, 2H, CH_2=), 7.84 (m, 2H, N−CH=CH−N), 9.32 (s, 1H, N−CH=N).

Synthesis of 1-(2-Methacryloyloxy)ethyl-3-butylimidazolium Bis(trifluoromethanesulfonyl)imide (MIS). A mixture of LiTFSI (87 mmol) and MIB (95 mmol) diluted with deionized water (130 mL) was stirred at 298 K for 36 h to induce a liquid−liquid phase separation. The organic layer containing the ionic liquid was isolated with a separating funnel and diluted with dichloromethane. The solution was washed with water three times, mixed with activated carbon powder, and allowed to stand in a light-resistant container overnight. After filtration, the product was concentrated by using an evaporator and was dried under reduced pressure to afford 39.8 g of MIS (77 mmol, 88%) as a viscous liquid. FW = 517.5. ^{1}H NMR (DMSO-d_6, 300 MHz): δ 0.87 (t, 3H, $NCH_2CH_2CH_2CH_3$), 1.20 (m, 2H, $NCH_2CH_2CH_2CH_3$), 1.74 (m, 2H, $NCH_2CH_2CH_2CH_3$), 1.82 (s, 3H, CH_3), 4.17 (t, 2H, OCH_2), 4.47 and 4.52 (q, 4H, $NCH_2CH_2CH_2CH_3$, OCH_2CH_2), 5.71 and 6.01 (s, 2H, CH_2=), 7.80 (m, 2H, N−CH=CH−N), 9.23 (s, 1H, N−CH=N); ^{13}C NMR (DMSO-d_6, 75 MHz): δ 13.4 ($NCH_2CH_2CH_2CH_3$), 18.0 ($NCH_2CH_2CH_2CH_3$), 18.8 (CH_3), 31.5 ($NCH_2CH_2CH_2CH_3$), 48.2 and 48.8 (NCH_2CH_2), 62.8 (OCH_2), 122.9 (CH_2=), 123.2 and 127.0 (N−CH=CH-N), 135.5 (CH_2=*C*), 137.1 (N−CH=N), 166.4 (C=O).

Polymer Brush Preparation. A few sheets of the BHE-immobilized silicon wafers, CuBr (0.045 mmol), and bpy (0.091 mmol) were introduced into a well-dried glass tube with a stopcock; the glass tube was degassed by seven cycles of vacuum pumping and flushing with argon. Degassed acetonitrile (4.4 mL), MIS (8.54 g, 17 mmol), and EB (free initiator, 0.025 mmol) in a separate Schlenk flask were added to a catalyst in the glass tube. The polymerization solution was degassed by repeatedly carrying out a freeze-and-thaw process to remove the oxygen. The polymerization reaction was conducted at 318 K for 73 h under argon to simultaneously generate the PMIS brush from the substrate and free PMIS from EB. The reaction was stopped by opening the glass vessel to air, and the reaction mixture was poured into chloroform to precipitate the free polymer. The polymer solution was passed through the alumina column using THF to remove the catalysts. The silicon wafers were washed with acetonitrile using a Soxhlet apparatus for 12 h to remove the free polymer adsorbed on their surfaces, and they were dried under reduced pressure for 2 h. The PHMA brush was also prepared in a similar manner.

Characterization. Size exclusion chromatography (SEC) of the free soluble PMIS was performed to determine the molecular weight and molecular weight distribution with a JASCO LC system connected to three PS gel columns of Shodex GF-310 HQ × 2 + GF-510 HQ and equipped with a multiangle light-scattering detector (MALS; Wyatt Technology DAWN-EOS, wavelength: λ = 690 nm) using methanol/water (9/1, v/v) containing acetic acid (0.5 M) and sodium nitrate (0.3 M) as an eluent at a rate of 0.6 mL min^{-1}. The DSC measurement was performed with the EXSTAR6000 (SEIKO Instruments Inc.) in a temperature range of 173 to 473 K at a heating rate of 10 K min^{-1}. The contact angles against water and diiodemethane were recorded with a drop shape analysis system, DSA10 Mk2 (KRÜSS Inc.), equipped with a video camera. XPS measurements were carried out on an XPS-APEX (Physical Electronics Co. Ltd.) at 1 × 10^{-6} Pa using a monochromatic Al−Kα X-ray source of 150 W. All of the XPS data were collected at a takeoff-angle of 45° and a low-energy (25 eV) electron flood gun was used to minimize sample charging. The survey spectra (0−1000 eV) and high-resolution spectra of the C_{1s}, O_{1s}, F_{1s}, N_{1s}, S_{2p}, and Si_{2p} regions were acquired at pass energies for the analyzer of 100.0 and 25.0 eV, respectively. An X-ray beam was focused onto an area with a diameter of ca. 0.2 mm. The calibrated atomic concentrations (AC) were calculated from the peak areas (A) of the high resolution spectra, considering the sensitivity factors (S) and measuring time (T) using the following equation:

$$\text{AC of element } x = [(A_x/S_xT_x)/\sum (A_i/S_iT_i)] \times 100 \quad (1)$$

The IR spectra of the polymer brushes grown on silicon substrates were measured in the transmission mode using a Spectrum One KY type (Perkin-Elmer) system coupled with an MCT-I detector. AFM observations and film thickness measurements were carried out with an SPI4000 (SII NanoTechnology Inc.) using an Si_3N_4 tip on a cantilever with a spring constant of 0.09 N m^{-1} at ambient pressure. The thickness of the polymer brush was determined by AFM scanning on the scratched surface of the polymer brush. Optical micrographs were obtained using an Eclipse E400 (Nikon Corporation).

Macroscopic friction tests on polymer brushes were carried out on a conventional ball-on-plate type reciprocating tribotester, Tribostation Type32 (Shinto Scientific Co. Ltd., Tokyo), by sliding a glass ball on the substrates at a reciprocating distance of 20 mm and a rate of 1.5 × 10^{-3} m s^{-1} in a dry nitrogen atmosphere, water, methanol, and EMImTFSI under a normal load of 0.49 N at room temperature. The friction force was measured by a strain gauge attached to the arm of the tester and was recorded as a function of time. The friction coefficient was given by the friction force divided by the normal load. Every friction test used a virgin surface area on the brush substrate to measure the friction coefficient of the first reciprocating scan of the sliding probe. The friction coefficients for at least five trials were stored and averaged. In the case of a bare silicon wafer, the friction coefficients of the fourth scan cycles were stored to avoid the influence of the oxide layer on the silicon surface. The substrate of the test piece was pinned by a PTFE belt and screws in a Teflon trough filled with an ionic liquid. The Teflon trough was fixed on a moving stage. In the case of a nonmodified silicon wafer under a normal load of 50 g (0.49 N), the theoretical contact area between the glass probe and substrate could be estimated to be 3.51 × 10^{-9} m^2 by Hertz's contact mechanics theory (46) and the average pressure on the contact area was estimated to be 139 MPa. Although the actual contact area and pressure on the brush surface cannot be estimated by Hertz's theory, the normal pressure would have been over 1 × 10^2 MPa in our experiments.

RESULTS AND DISCUSSIONS

Preparation of PMIS Brush. The SI-ATRP of MIS at 318 K from the initiator-immobilized silicon wafer proceeded slowly for 3 days to yield a PMIS brush with a thickness of 54 nm, as shown in Scheme 2. The formation

Scheme 2. Surface-Initiated ATRP of MIS from Initiator-Immobilized Silicon Wafer

of the PMIS brush was also confirmed by XPS, as shown in Figure 1. Peaks corresponding to the C−C, C−O (C−N), C═O, and CF_3 bonds appeared at 285.0, 286.5, 288.8, and 292.5 eV, respectively. The N_{1s} spectrum exhibited two peaks at 399.2 and 401.8 eV attributed to the sulfonylimide and imidazorium units. The F_{1s} and $S_{2p(3/2)}$ peaks of sulfonylimide anions were observed at 688.5 and 168.4 eV. The surface atomic ratios of carbon, oxygen, fluorine, nitrogen, and sulfur observed by XPS revealed good agreement with the theoretical values calculated from the atomic composition of MIS. The AFM observation revealed that a homogeneous polymer layer was formed on the substrate, and the surface roughness was 0.5 nm in the vacuum state in a 5 × 5 μm^2 scan area. A 60 nm thick PHMA brush was also prepared by a similar SI-ATRP protocol.

SI-ATRP in the presence of the free initiator simultaneously produced a polymer brush and a free (unbound) polymer. The number-average molecular weight (M_n) value of PMIS estimated by MALS-SEC was 316000, and the polydispersity index (M_w/M_n) of the free PMIS obtained was 1.65. The M_n of the surface-grafted polymer on the silicon wafer was not directly determined here, but it is generally accepted that a polymer brush has the same molecular weight as the corresponding free polymer (47−50). The free PMIS was a highly viscous polymer at room temperature because the glass transition temperature (T_g) was 268.5 K, which is very close to the T_g of PHMA (268.0 K) (51). The free PMIS obtained dissolved well in acetone, acetonitrile, methanol, and EMImTFSI but was insoluble in water and diiodemethane.

The relationship between the solubility of PMIS and the friction properties of the brush is important, as will be described below. The thicknesses of the polymer brushes on the silicon substrates were evaluated primarily by an imaging ellipsometer equipped with a YAG laser (532.8 nm). The graft density, σ, of the PMIS brush was estimated to be 0.14 chains nm^{-2} based on the relationship between the thickness L (nm) and M_n, as follows (49):

$$\sigma = dLN_A \times 10^{-21}/M_n \qquad (2)$$

where d and N_A are the assumed density of bulk polymer at 293 K and Avogadro's number, respectively. This value is lower than the typical graft density of a PMMA brush (0.60−0.70 chains nm^{-2}) or a PHMA brush (0.56 chains nm^{-2}) prepared by the "grafting-from" method, because PMIS has a bulky imidazolium group at the side chain, which occupies a large cross-sectional area on the surface. The contact angles against water and diiodemethane were 79 and 68°, respectively, as listed in Table 1. The surface free energy calculated by Owens' protocol (52) was 30.1 mJ m^{-2}. The contact angle of the EMImTFSI on the PMIS brush surface was 10° within 1 min after the EMImTFSI was dropped. However, the ionic liquid spread continuously and swelled the brush (53), and the contact angle reached nearly 0° within 10 min. This result indicated the excellent affinity of the PMIS brush to EMImTFSI.

Table 1. Static Contact Angles of Polymer Brushes

	contact angle (deg)		surface free energy (mJ m^{-2})		
samples	water[a]	CH_2I_2 [a]	γ_s^d	γ_s^p	γ_s
PMIS brush	79	68	20.1	10.0	30.1
PMIS spin-cast film	84	71	18.8	8.0	26.9
PHMA brush	92	74	18.4	4.7	23.0

[a] 2.0 μL.

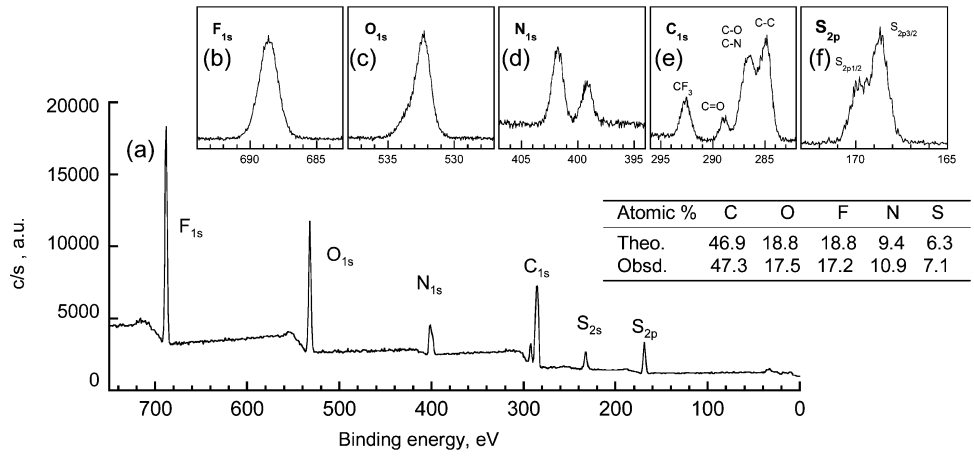

FIGURE 1. XPS spectra of PMIS brush surface: (a) survey scan spectrum; high-resolution spectra of (b) F_{1s}, (c) O_{1s}, (d) N_{1s}, (e) C_{1s}, (f) S_{2p} peak region.

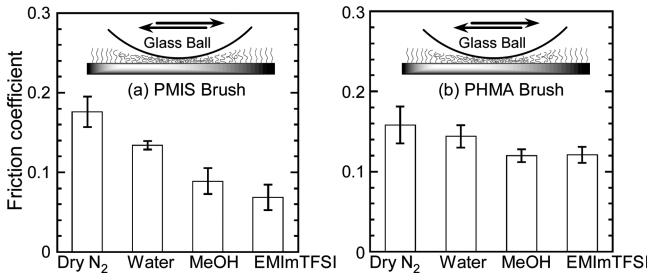

FIGURE 2. Friction coefficient of (a) PMIS and (b) PHMA brushes in dry N_2 atmosphere, water, methanol, and EMImTFSI by sliding a glass ball over a distance of 20 mm at a sliding velocity of 1.5×10^{-3} m s^{-1} under a normal load of 0.49 N at 298 K.

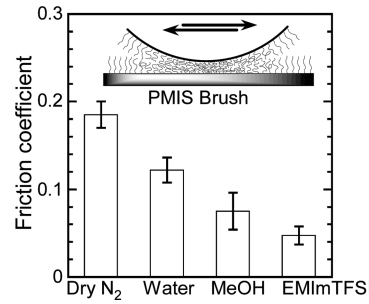

FIGURE 3. Friction coefficient of PMIS and PHMA brushes in dry N_2 atmosphere, water, methanol, and EMImTFSI by sliding a glass ball immobilized with PMIS brush over a distance of 20 mm at a sliding velocity of 1.5×10^{-3} m s^{-1} under a normal load of 0.49 N at 298 K.

Frictional Properties of the PMIS Brush. Figure 2 shows the friction coefficients of the PMIS and PHMA brushes measured by sliding a friction probe over a distance of 20 mm at a sliding velocity of 1.5×10^{-3} m s^{-1} in a dry nitrogen atmosphere, water, methanol, and EMImTFSI at 298 K. A high friction coefficient was observed under the dry N_2 condition, whereas lower friction coefficients were observed in the water and organic solvent due to the fluid lubrication effect. The friction coefficient of the nonmodified silicon wafer was larger than 0.2 in the dry N_2 atmosphere, although the value is not shown in Figure 2. It is notable that the friction coefficient appears to be dependent on the solvent quality. A remarkable reduction in the friction coefficient was observed for the PMIS brush in methanol and EMImTFSI, which are good solvents for PMIS, whereas a two-times-higher friction coefficient was observed in water, which is a poor solvent for PMIS.

The effect of the solvent quality on the friction coefficients of polymer brushes in various solvents has been previously reported. When the solvent was changed from an good solvent to a theta solvent, Kilbey et al. observed larger shear forces between sliding surfaces immobilized with PS brushes using SFA (30, 36). Spencer et al. observed that the friction coefficient of a poly(ethylene glycol) (PEG) brush surface in water, measured by colloidal-probe lateral force microscopy, increased from 0.2 to 0.6 when the volume fraction of 2-propanol exceeded 85% (54). They found that a hydrated PEG brush in water adopted an extended chain conformation to afford effective boundary lubricants, whereas an increase in the 2-propanol fraction resulted in the collapse of the brushlike structure to a more random-coil-like polymer conformation. Tsujii and his co-workers reported that an extraordinarily low friction coefficient was observed by an LFM study of a high-density PMMA brush in toluene (37) because of the large osmotic pressure and configurational entropy effects. Similar trends can be also seen in a macroscopic frictional test. High-density PMMA brushes in toluene and acetone revealed lower friction coefficients than in hexane and cyclohexane when a stainless steel ball was used as a sliding probe (39). Hydrophilic poly(2,3-dihydroxypropyl methacrylate) (43) and poly(2-methacryloyloxyethyl phosphorylcholine) (44) showed lower friction coefficients in good solvents such as water, but showed higher values in poor solvents such as toluene.

Therefore, the magnitude of the polymer/solvent interaction must have played an important role in the solvent quality effect. In this study, EMImTFSI and methanol were regarded as good solvents whereas water was inferior in quality with respect to PMIS. A PMIS brush would be highly solvated with EMImTFSI to form a swollen boundary layer. EMImTFSI would moderate the interaction between the brush surface and a glass ball probe to give a lower friction coefficient. In contrast, the PMIS chains in water would be unwilling to be in contact with water molecules, but prefer to interact with the polymers or friction probe rather than solvent molecules, thus giving a higher friction coefficient. A similar trend was observed with the PHMA brush. Water, methanol, and EMImTFSI are poor solvents for PHMA. Therefore, the friction coefficient of the PHMA brush was not as reduced, even in EMImTFSI. These results indicated that the imidazolium moiety in the polymer brush contributed to the reduction in the friction coefficient, especially when combined with an ionic liquid. Here, we note that the PHMA brush also showed a much lower friction coefficient, 0.05, in an good solvent such as toluene.

The friction coefficient of the PMIS brush was further reduced when a PMIS brush-immobilized glass probe was used as the sliding probe, as shown in Figure 3. For instance, the brush-vs-brush friction coefficient in an ionic liquid was 0.048, which was lower than that of the brush-vs-glass (0.078). We supposed that this reduction in the friction coefficient was caused by a thicker boundary film produced by the swollen brush and high osmotic pressure from densely grafted polymer chains with the approach of polymer brush bearing surfaces.

The friction force as a function of the normal load for the PMIS brush vs PMIS brush system is shown in Figure 4. The friction force of the PMIS brush was measured by sliding a PMIS brush-immobilized glass ball on a flat silicon substrate bearing the PMIS brush over a distance of 20 mm at a sliding velocity of 1.5×10^{-3} m s^{-1} in EMImTFSI at 298 K. The brush-immobilized substrate was immersed in EMImTFSI and was allowed to equilibrate for 1 h before the friction test. Under a normal load in the range of 0.2−0.98 N, an almost linear relation was observed between the load and the friction forces, with a friction coefficient of 0.048. However, a slightly larger friction coefficient was observed at a higher normal load of 1.96 N. This friction system between the

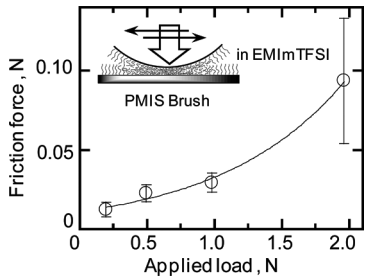

FIGURE 4. Dependence of friction force vs normal load for PMIS brush on silicon wafer by sliding a PMIS brush-immobilized glass ball in EMImTFSI over a distance of 20 mm at a sliding velocity of 1.5×10^{-3} m s^{-1} under a normal load of 0.20−1.98 N at 298 K.

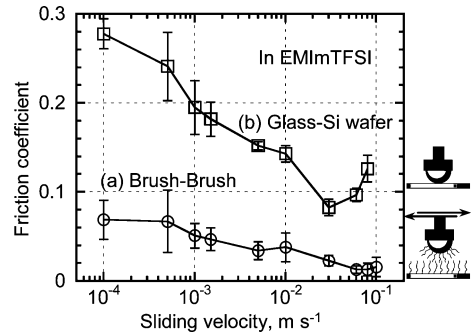

FIGURE 5. Sliding velocity dependence of the friction coefficient of (a) PMIS brush vs. PMIS brush and (b) glass ball vs silicon wafer in EMImTFSI under a normal load of 0.49 N at 298 K.

brushes did not seem to obey Amonton's law, $F = \mu W$, which indicates that the friction force, F, is linearly proportional to the load, W. If the friction system obeyed Amounton's law, friction force would not depend on the apparent contact area of the two solid surfaces or the sliding velocity. The brush film was thought to be largely deformed or partially collapsed by a normal pressure over 220 MPa, which was much higher than the osmotic pressure of the swollen brush in an ionic liquid.

The polymer concentration in a swollen brush was estimated as follows. It is well-known that a densely grafted polymer brush in a good solvent takes on an almost fully stretched conformation (55). Theoretically, the equilibrium thickness of solvent-swollen brushes is determined by the balance between the osmotic pressure and the stress induced by chain stretching. In fact, there have been many reports indicating that the thickness of a swollen brush with high graft density is fairly close to the full length of the graft chain in the all-trans conformation (56−58). Assuming that the contour length of the PMIS with $M_n = 316\,000$, consisting of ca. 610 monomer units, is equal to the swollen brush thickness, L' (nm), the polymer concentration, C (mol L^{-1}), in the swollen brush can be estimated by the following equation

$$C = (\sigma/N_A)(1 \times 10^{24}/L') \quad (3)$$

If we use 0.25 nm for the chain contour length per monomer unit, 0.14 chains nm^{-2} for the graft density, and 152 nm for L', C would be 1.5×10^{-3} (mol L^{-1}), which is equal to 35 wt %. We suppose that the osmotic pressure of the swollen PMIS brush in the ionic liquid is approximately 1−10 MPa, although this estimation is based on many assumptions.

Figure 5 displays the sliding velocity dependences of the friction coefficients of the PMIS brush surface and nonmodified silicon wafer surface in an ionic liquid. The friction coefficients at each sliding velocity were measured on a virgin surface area of the brush and silicon substrate. It can be seen that the friction coefficients of the silicon wafer were much higher than the PMIS brush surface in the range of 1×10^{-4}− to 1×10^{-1} m s^{-1}. The decrease in the friction coefficient with an increase in the sliding velocity was observed in both the brush-on-brush and glass-on-silicon friction systems. The friction coefficient of the silicon wafer gradually decreased from 0.3 to 0.08 when the sliding velocity increased from 1×10^{-4} to 2×10^{-2} m s^{-1} and increased with a further increase in sliding velocity after 2×10^{-2} m s^{-1}. In contrast, the friction coefficient of the PMIS brush gradually and continuously decreased from 0.07 to 0.01 with an increase in the sliding velocity over a wide range of 1×10^{-4} to 1×10^{-1} m s^{-1}. Making a comparison to the Stribeck curve (59), the decreasing friction with increasing velocity suggests that this system is in the mixed lubrication region. In the case of a low sliding rate, the interaction between the polymer brushes and their interpenetration dominated the friction to give a large friction coefficient (boundary or interfacial friction). With an increase in the sliding velocity, a thicker liquid layer would be formed between the sliding surfaces by the hydrodynamic lubrication effect to reduce the actual contact area and the friction force (mixed lubrication region). At higher sliding rates (or viscosities or pressures), the Stribeck curve will move to the elastohydrodynamic and hydrodynamic regions, and we would expect an increase in the friction force with the rate due to the shear resistance of the fluids. Unfortunately, in our experiments, the friction coefficients could not be measured at sliding rates much faster than 1×10^{-1} m s^{-1} because of the mechanical time constant of the tribometer. In a future study, we will measure the dependence of the friction force on the sliding velocity under a different normal load and temperature to detect and confirm the transition point of the lubrication regime for a PMIS brush in an ionic liquid.

Figure 6 shows the variations in the friction coefficients of the PMIS brush and PHMA brush in a dry nitrogen atmosphere with the number of friction cycles. The friction coefficient of the PHMA brush film began to increase in the early stage of the friction test, attaining a magnitude of 0.12 within 150 tracking cycles. This result indicates that the PHMA brush was abraded away by the sliding glass probe. In contrast, the relatively low friction coefficient of the high-density PMIS brush was continuously observed, as shown in curve (a) of Figure 6, implying a better wear resistance compared with the PHMA brush. Actually, the high-density PMIS brush maintained a friction coefficient of around 0.13 even after 800 friction cycles.

Figure 7 displays an optical microscope image of the wear track after 400 cycles of friction testing by the glass probe

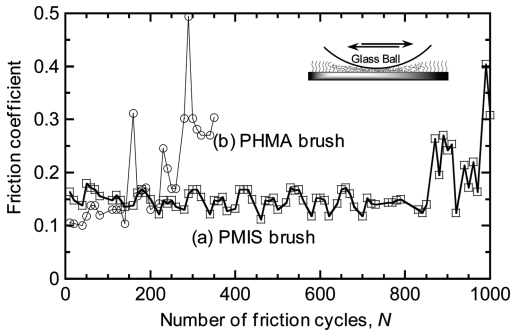

FIGURE 6. Variations of friction coefficient with the number of friction cycles *N* for the surface of (a) PMIS brush and (b) PHMA brush at a sliding velocity of 1.0×10^{-2} m s^{-1} under a normal load of 1.96 N in a dry N_2 atmosphere.

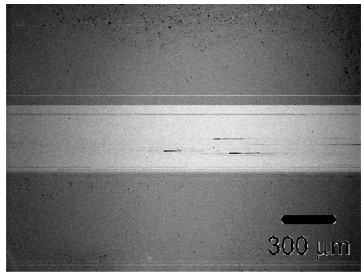

FIGURE 7. Optical microscope image of the wear track of the PMIS brush surface after 400 friction cycles by glass ball probe sliding at a sliding velocity of 1.0×10^{-2} m s^{-1} under a normal load of 1.96 N in a dry N_2 atmosphere at 298 K.

Table 2. Atomic Ratios of PMIS Brush and Its Worn Surfaces after Reciprocating Friction Test[a]

friction cycles (N)	atomic ratio[b] (%)						
	C_{1s}	O_{1s}	F_{1s}	N_{1s}	S_{2p}	Si_{2p}	C/Si
0	47.7	17.5	17.2	9.8	6.4	1.5	31.8
200	46.0	19.4	15.6	9.2	6.0	3.7	12.4
400	43.5	20.6	16.0	9.5	6.2	4.2	10.3
1000	14.8	36.4	3.9	2.9	7.1	34.8	0.4

[a] Friction test was conducted by glass ball probe sliding at a sliding velocity of 1.0×10^{-2} m s^{-1} under a load of 1.96 N in a dry N_2 atmosphere. [b] Surface atomic ratios were determined by high-resolution spectra of XPS.

sliding at a sliding velocity of 1.0×10^{-2} m s^{-1} in a dry N_2 atmosphere at 298 K. The worn surfaces inside the wear tracks were analyzed by XPS. Table 2 lists the atomic ratios of carbon, silicon, oxygen, fluorine, nitrogen, sulfur, and silicon in the worn surfaces before and after 200, 400, and 1000 friction cycles. With an increase in the number of friction cycles, the atomic ratio of the oxygen and silicon increased slightly, probably because of the reduction of the brush thickness. Remarkable differences were not observed in the atomic ratios for C_{1s}, F_{1s}, N_{1s}, and S_{2p} until 400 friction cycles. As shown in Figure 8, the C_{1s} spectra on the worn surfaces showed similar peak patterns before and after 200 and 400 friction cycles, indicating that the chemical structure of PMIS still remained. However, the atomic ratio of carbon and silicon (C_{1s}/Si_{2p}) considerably decreased from 31.8 to 0.4 after 1000 friction cycles. Because the Si_{2p} peak was attributed to the substrate, the reduction in the C_{1s}/Si_{2p} value indicated that the 40-nm thick PMIS brush was gradually abraded away with increasing friction cycles of reciprocating sliding of the glass ball probe, and was finally peeled off after 1000 friction cycles. The atomic ratio of carbon and fluorine decreased drastically after 1000 friction cycles, whereas the sulfur component still remained on the worn surface. The peak intensity at 294 eV attributed to CF_3 apparently decreased compared with the three peaks at 285−290 eV corresponding to C═O, C−O, C−N, and C−C binding energies, as shown in Figure 8d. These results revealed that the chemical decomposition of the PMIS and counteranions took place after the brush layer peeled off. Further precise analyses of the worn surfaces are in progress.

As mentioned in the Introduction, the tribological properties of an ionic liquid largely depend on counteranions. Minami (60) and Itoh et al. (61) reported observing excellent tribological properties when using hydrophobic anions, such as trifluorotris(pentafluoroethyl) phosphate and perfluoroalkyl sulfate, probably because the low moisture content of ionic liquids retards unfavorable chemical reactions. In this work, only TFSI was investigated as a counteranion for an imidazolium-type poly(ionic liquid). Further improvement of the tribological properties of poly(ionic liquids) could be expected by optimizing the combination of organic anions and cations.

CONCLUSIONS

In this paper, we have reported the tribological properties of a poly(ionic liquid) brush and have compared the brush with a nonionic PHMA brush. The PMIS brush showed a friction coefficient of around 0.13 even after 800 cycles of reciprocating sliding of a glass ball probe under a dry nitrogen atmosphere, whereas the PHMA brush showed a

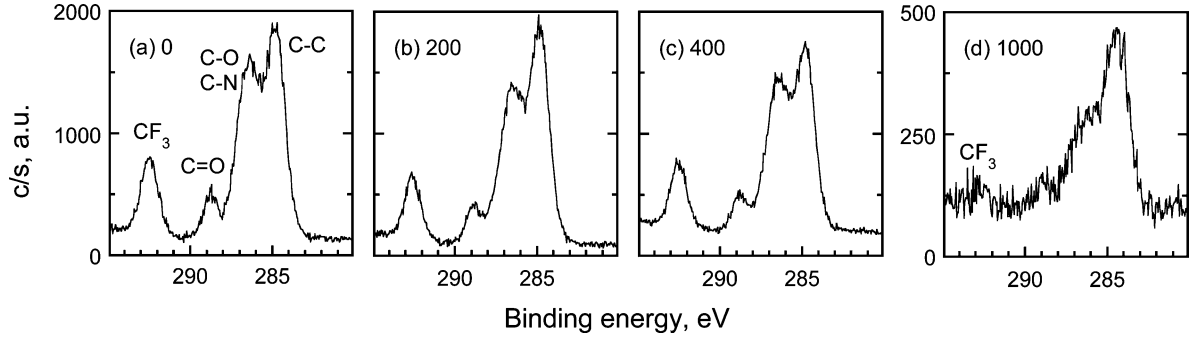

FIGURE 8. XPS spectra of C_{1s} of worn surface of the PMIS brush after friction cycles of (a) 0, (b) 200, (c) 400, and (d) 1000 by glass ball probe sliding at a sliding velocity of 1.0×10^{-2} m s^{-1} under a load of 1.96 N in dry N_2 atmosphere.

friction coefficient much higher than 0.3 within 100 friction cycles because the brush wore out. These results indicated that the poly(ionic liquid) brush contributed to the formation of a good lubricant layer. In addition, we showed that the combination of a poly(ionic liquid) brush and an ionic liquid displayed a low friction coefficient. The influences of solvent quality on the tribological properties have been well studied, and in general, a polymer brush immersed in a good solvent would afford an extremely low friction coefficient. A similar effect can be considered for the combination of a PMIS brush and EMImTFSI. There are several reasons for the reduction in the friction coefficient achieved by a swollen PMIS brush and EMImTFSI. First, the PMIS brush was strongly tethered to the substrate by covalent bonds. In addition, the PMIS brush surface had good wettability and high affinity for the ionic liquid, which enabled the EMImTFSI to spread and permeate into the PMIS brush, forming a good lubrication film and reducing the molecular interaction between opposite sliding brushes. The high viscosity of the swollen brush film in EMImTFSI also contributed to maintaining the lubrication film, even under severe friction conditions. In contrast, the PMIS brush immersed in a poor solvent such as water showed a larger friction coefficient. The affinity of the polymer brush for the solvent (or lubricant) plays an important role in controlling the interaction between the brush and the friction probe, as well as the frictional properties. XPS analysis of the wear tracks revealed that the PMIS brush layer was gradually abraded away by sliding a glass ball probe in a N_2 atmosphere under a normal load of 1.96 N, and the layer was peeled off after 1000 friction cycles, which resulted in a much higher friction coefficient. Further improvement in the wear resistance is necessary before a PMIS brush can be put to practical use.

Acknowledgment. The present work is supported by a Grant-in-Aid for the Global COE Program, "Science for Future Molecular Systems", and partially supported by a Grant-in Aid for Young Scientist (B) (19750098) from the Ministry of Education, Culture, Science, Sports and Technology of Japan. We gratefully acknowledge Idemitsu Kosan Co. Ltd. for supply of ionic liquids.

REFERENCES AND NOTES

(1) Ye, C.; Liu, W.; Chen, Y.; Yu, L. *Chem. Commun.* **2001**, 2244–2245.
(2) Liu, W.; Ye, C.; Gong, Q.; Wang, H.; Wang, P. *Tribol. Lett.* **2002**, *13*, 81–85.
(3) Liu, W.; Ye, C.; Chen, Y.; Ou, Z.; Sun, D. C. *Tribol. Int.* **2002**, *35*, 503–509.
(4) Jiménez, A. E.; Bermúdez, M. D.; Carrióna, F. J.; Martínez-Nicolás, G. *Wear* **2006**, *261*, 347–359.
(5) Phillips, B. S.; John, G.; Zabinski, J. S. *Tribol. Lett.* **2007**, *26*, 85–91.
(6) Jin, C.-M.; Ye, C.; Phillips, B. S.; Zabinski, J. S.; Liu, X.; Liu, W.; Shreeve, J. M. *J. Mater. Chem.* **2006**, *16*, 1529–1535.
(7) Suzuki, A.; Shinka, Y.; Masuko, M. *Tribol. Lett.* **2007**, *27*, 307–313.
(8) Wilkes, J. S.; Zaworotko, M. J. *Chem. Commun.* **1992**, 965–966.
(9) Bermúdez, M. D.; Jiménez, A. E.; Sanes, J.; Carrión, F. J. *Molecules* **2009**, *14*, 2888–2908.
(10) Zhou, F.; Liang, Y.; Liu, W. *Chem. Soc. Rev.* **2009**, *38*, 2590–2599.
(11) Minami, I. *Molecules* **2009**, *14*, 2286–2305.
(12) Kamimura, H.; Chiba, T.; Watanabe, N.; Kubo, T.; Nakano, H.; Minami, I.; Mori, S. *Tribol. Online* **2006**, *1*, 40–43.
(13) Kamimura, H.; Kubo, T.; Minami, I.; Mori, S. *Tribol. Int.* **2007**, *40*, 620–625.
(14) Minami, I.; Watanabe, N.; Nanao, H.; Mori, S.; Fukumoto, K. *J. Synth. Lubr.* **2008**, *25*, 45–55.
(15) Jiménez, A. E.; Bermúdez, M. D. *Tribol. Lett.* **2007**, *26*, 53–60.
(16) Phillips, B. S.; Zabinski, J. S. *Tribol. Lett.* **2004**, *17*, 533–541.
(17) Jiménez, A. E.; Bermúdez, M. D.; Iglesias, P.; Carrión, F. J.; Martínez-Nicolás, G. *Wear* **2006**, *260*, 766–782.
(18) Sanes, J.; Carrion, F. J.; Bermúdez, M. D.; Martínez-Nicolás, G. *Tribol. Lett.* **2006**, *21*, 121–133.
(19) Kobayashi, M.; Ishida, H.; Kaido, M.; Suzuki, A.; Takahara, A. In *Surfactants in Tribology Frictional Properites of Organosilane Monolayers and High-density Polymer Brushes*; Biresaw, G., Mittal, K. L., Eds.; CRC Press: Boca Raton, FL, 2008; pp89−110.
(20) Kobayashi, M.; Wang, Z.; Matsuda, Y.; Kaido, M.; Suzuki, A.; Takahara, A. Tribological Behavior of Polymer Brush Prepared by the Grafting-from Method. In *Polymer Tribology*; Kumar, S. S., Ed.; Imperial College Press: London, 2009; pp582−602.
(21) Ishida, H.; Koga, T.; Morita, M.; Otsuka, H.; Takahara, A. *Tribology Lett.* **2005**, *19*, 3–8.
(22) Advincula, R. C.; Brittain, W. J.; Caster, K. C.; Rühe, J. *Polymer Brushes*; Wiley-VCH: Weinheim, Germany, 2004.
(23) Miklavic, S. J.; Marčelja, S. *J. Phys. Chem.* **1988**, *92*, 6718–6722.
(24) Fredrickson, G. H.; Pincus, P. *Langmuir* **1991**, *7*, 786–795.
(25) Halperin, A.; Tirrell, M.; Lodge, T. P. *Adv. Polym. Sci.* **1992**, *100*, 31–71.
(26) Klein, J.; Kumacheva, E.; Mahalu, D.; Perahia, D.; Fetters, L. *Nature* **1994**, *370*, 634–636.
(27) Klein, J. *Annu. Rev. Mater. Sci.* **1996**, *26*, 581–612.
(28) Taunton, H. J.; Toprakcioglu, C.; Fetters, L. J.; Klein, J. *Nature* **1988**, *332*, 712–714.
(29) Witten, T. A.; Leibler, L.; Pincus, P. A. *Macromolecules* **1990**, *23*, 824–829.
(30) Schorr, P. A.; Kwan, T. C. B.; Kilbey II, S. M.; Shaqfeh, E. S. G.; Tirrell, M. *Macromolecules* **2003**, *36*, 389–398.
(31) Tadmor, R.; Janik, J.; Klein, J.; Fetters, L. J. *Phys. Rev. Lett.* **2003**, *91*, 115503.
(32) Grest, G. S. *Adv. Polym. Sci.* **1999**, *138*, 149–183.
(33) Kreer, T.; Müser, M. H.; Binder, K.; Klein, J. *Langmuir* **2001**, *17*, 7804–7813.
(34) Klein, J.; Kumacheva, E.; Perahia, D.; Fetters, L. J. *Acta Polym.* **1998**, *49*, 617–625.
(35) Dhinojwala, A.; Granick, S. *Macromolecules* **1997**, *30*, 1079–1085.
(36) Forster, A. M.; Mays, J. W.; Kilbey II, S. M. *J. Polym. Sci., Part B: Polym. Phys.* **2006**, *44*, 649–655.
(37) Tsujii, Y.; Okayasu, K.; Ohno, K.; Fukuda, T. *Polym. Prepr. (Am. Chem. Soc., Div. Polym. Chem.)* **2005**, *46* (2), 85.
(38) Yamamoto, S.; Ejaz, M.; Tsujii, Y.; Fukuda, T. *Macromolecules* **2000**, *33*, 5608–5612.
(39) Sakata, H.; Kobayashi, M.; Otsuka, H.; Takahara, A. *Polym. J.* **2005**, *37*, 767–775.
(40) Yu, B.; Zhou, F.; Hu, H.; Wang, C.; Liu, W. *Electrochim. Acta* **2007**, *53*, 487–494.
(41) He, X.; Yang, W.; Pei, X. *Macromolecules* **2008**, *41*, 4615–4621.
(42) Ohno, K.; Morinaga, T.; Koh, K.; Tsujii, Y.; Fukuda, T. *Macromolecules* **2005**, *38*, 2137–2142.
(43) Kobayashi, M.; Takahara, A. *Chem. Lett.* **2005**, *34*, 1582–1583.
(44) Kobayashi, M.; Terayama, Y.; Hosaka, N.; Kaido, M.; Suzuki, A.; Yamada, N.; Torikai, N.; Ishihara, K.; Takahara, A. *Soft Matter* **2007**, *3*, 740–746.
(45) Hayashi, K.; Saito, N.; Sugimura, H.; Takai, O.; Nagagiri, N. *Langmuir* **2002**, *18*, 7469–7472.
(46) If a circle with radius a (m) is regarded as the contact area between a glass ball and substrate under a normal load P (0.49 N), Hertz's theory affords the following relationship using Young's modulus of glass and silicon wafer, E_A (7.16×10^{10} Pa), E_B (1.30×10^{11} Pa), and Poisson's ratio υ_A (0.23), υ_B (0.28), respectively: $2/E = (1-\upsilon_A^2)/E_A + (1-\upsilon_B^2)/E_B$ and $a = ((3/4)(2/E)PR_A)^{1/3}$, where R_A is the curvature radius (5.00×10^{-3} m) of glass ball. The contact area can be calculated by πa^2.
(47) Matsuno, R.; Yamamoto, K.; Otsuka, H.; Takahara, A. *Macromolecules* **2004**, *37*, 2203–2209.
(48) Werne, T. v.; Patten, T. E. *J. Am. Chem. Soc.* **1999**, *121*, 7409–7410.
(49) Husseman, M.; Malmstrom, E. E.; McNamura, M.; Mate, M.; Mecerreyes, D.; Benoit, D. G.; Hedrick, J. L.; Mansky, P.; Huang,

E.; Russell, T. P.; Hawker, C. J. *Macromolecules* **1999**, *32*, 1424–1431.
(50) Pyun, J.; Jia, S.; Kowalewski, T.; Patterson, G. D.; Matyjaszewski, K. *Macromolecules* **2003**, *36*, 5094–5104.
(51) Meier, G.; Kremer, F.; Fytas, G.; Rizos, A. *J. Polym. Sci., Part B: Polym. Phys.* **1996**, *34*, 1391–1401.
(52) Owens, D. K.; Wendt, R. C. *J. Appl. Polym. Sci.* **1969**, *13*, 1741–1747.
(53) Stuart, M. A. C.; de Vos, W. M.; Leernakers, F. A. M. *Langmuir* **2006**, *22*, 1722–1728.
(54) Miller, M. T.; Yan, X.; Lee, S.; Perry, S. S.; Spencer, N. D. *Macromolecules* **2005**, *38*, 3861–3866.
(55) Yamamoto, S.; Ejaz, M.; Tsujii, Y.; Matsumoto, M.; Fukuda, T. *Macromolecules* **2000**, *33*, 5602–5607.
(56) Wu, T.; Efimenko, K.; Vlček, P.; Šubr, V.; Genzer, J. *Macromolecules* **2003**, *36*, 2448–2453.
(57) Tsujii, Y.; Ohno, K.; Yamamoto, S.; Goto, A.; Fukuda, T. *Adv. Polym. Sci.* **2006**, *197*, 1–45.
(58) Kobayashi, M.; Terayama, Y.; Hino, M.; Ishihara, K.; Takahara, A. *J. Phys.: Conf. Ser.* **2009**, *184*, 012010.
(59) Spikes, H. A. Boundary Lubrication and Boundary Films. *The Films in Tribology*; Dowson, D., Talor, C. M., Childs, T. H. C.,Godet, M., Dalmz, G., Eds.; Elsevier: New York, 1993; pp331−346.
(60) Minami, I.; Kita, M.; Kubo, T.; Nanao, H.; Mori, S. *Tribol. Lett.* **2008**, *30*, 215–223.
(61) Itoh, T.; Watanabe, N.; Inada, K.; Ishioka, A.; Hayase, S.; Kawatsura, M.; Minami, I.; Mori, S. *Chem. Lett.* **2009**, *38*, 64–65.

AM9009082